Journal of Materials Chemistry A

PAPER

View Article Online
View Journal | View Issue

Cite this: J. Mater. Chem. A, 2016, 4, 3027

Flux-mediated doping of $SrTiO_3$ photocatalysts for efficient overall water splitting†

Yeilin Ham,[a] Takashi Hisatomi,‡[a] Yosuke Goto,[a] Yosuke Moriya,‡[a] Yoshihisa Sakata,[b] Akira Yamakata,[c] Jun Kubota[d] and Kazunari Domen‡*[a]

Received 30th June 2015
Accepted 25th September 2015

DOI: 10.1039/c5ta04843e

www.rsc.org/MaterialsA

$SrTiO_3$ is a photocatalyst that is well known for its activity for the overall water splitting reaction under UV light irradiation. In this study, the effects of $SrCl_2$ flux treatments and Al doping on the photocatalytic properties of $SrTiO_3$ were investigated. The $SrTiO_3$, which showed an apparent quantum efficiency of 30% at 360 nm in the overall water splitting reaction, the highest value reported so far, was prepared by $SrCl_2$ flux treatments in alumina crucibles. Scanning electron microscopy and X-ray diffractometry revealed that the flux-treated $SrTiO_3$ consisted of well-crystalline particles with a cubic shape reflecting the perovskite-type structure. Inductively coupled plasma optical emission spectroscopy revealed that Al ions from the alumina crucibles were incorporated into the $SrTiO_3$ samples. The $SrTiO_3$ that was treated with $SrCl_2$ flux in Al-free conditions showed a marginal improvement in photocatalytic activity despite the high crystallinity and the clear crystal habit. Doping $SrTiO_3$ with Al improved the photocatalytic activity even without $SrCl_2$ treatment. These results suggested that Al doping was a principal factor in the dramatic improvement in the water splitting activity of the flux-treated $SrTiO_3$. The effects of flux treatments and Al doping on the morphology and water splitting activity of $SrTiO_3$ were discussed separately.

1 Introduction

Photocatalytic water splitting is a promising technology for the utilization of solar energy in the production of renewable hydrogen.[1–4] In the last four decades, a number of particulate photocatalysts capable of overall water splitting have been developed.[1] La-doped $NaTaO_3$ loaded with NiO has reportedly split water at an apparent quantum efficiency of 56% at 270 nm.[5] Zn-doped Ga_2O_3 loaded with $Rh_{2-y}Cr_yO_3$ has also been reported to split water at a high reaction rate.[6] Some layered oxides such as $K_4Nb_6O_{17}$,[7] $Rb_4Nb_6O_{17}$,[8] and $Rb_2La_2Ti_3O_{10}$ (ref. 9) are known to show relatively high apparent quantum efficiencies (5%, 10%, and 5%, respectively) at 330 nm when modified with appropriate cocatalysts. However, these materials are active only under UV light, limiting their application to solar energy conversion. The highest apparent quantum efficiency recorded in the visible light region was 5.1% (at 410 nm), attained by $Rh_{2-y}Cr_yO_3/(Ga_{1-x}Zn_x)(N_{1-x}O_x)$.[3] It is necessary to develop effective methods to improve the apparent quantum efficiency at wavelengths to achieve a solar-to-hydrogen energy conversion efficiency of 5–10%, which has been targeted for cost-competitive production of solar hydrogen *via* photocatalytic water splitting.[3,4,10]

Given a specific photocatalytic material, controlling charge separation and migration is critical because the band structure and crystallographic character of each semiconducting material are unique. The movement of excited electrons and holes, and thus the photocatalytic activity, can be greatly affected by the crystallinity, particle size, and doping. Higher crystallinity and smaller particle sizes are desirable for charge migration toward surface active sites before recombination. Highly crystalline particles can be obtained by using a flux as a growth medium. The flux method, which allows the growth of crystalline particles *via* dissolution and recrystallization of solutes driven by supersaturation, has been applied to the synthesis of metal oxides,[11] including semiconducting oxides, such as $K_4Nb_6O_{17}$,[12] KNb_3O_8,[13] $Na_2Ti_6O_{13}$,[14] $K_2Ti_6O_{13}$,[15] and $SnNb_2O_6$.[16] Some of these oxides showed improved photocatalytic activity compared to those prepared by other synthesis methods. Some semiconducting (oxy)nitride photocatalysts such as $LaTiO_2N$,[17] C_3N_4,[18] and Ta_3N_5 (ref. 19) have also been prepared with the aid of a

[a]Department of Chemical System Engineering, School of Engineering, The University of Tokyo, 7-3-1 Hongo, Bunkyo-ku, Tokyo 113-8656, Japan. E-mail: domen@chemsys.t.u-tokyo.ac.jp; Fax: +81 03 5481 8838; Tel: +81 03 5481 1652

[b]Graduate School of Science and Engineering, Yamaguchi University, 2-16-1 Tokiwadai, Ube-shi, Yamaguchi 755-8611, Japan

[c]Graduate School of Engineering, Toyota Technological Institute, 2-12-1 Hisakata, Tempaku, Nagoya 468-8511, Japan

[d]Department of Chemical Engineering, Fukuoka University, 19-1 Nanakuma 8-Chome, Jonan-ku, Fukuoka, 814-0180 Japan

† Electronic supplementary information (ESI) available: DR spectra, XRD patterns, SEM images, and photocatalytic activity of the samples. See DOI: 10.1039/c5ta04843e

‡ Japan Technological Research Association of Artificial Photosynthetic Chemical Process (ARPChem), 5-1-5 Kashiwanoha, Kashiwa-shi, 277-8589 Chiba, Japan.

flux. However, the downside of this method is the incorporation of impurities into the target material, a commonly observed phenomenon during flux treatment.[20] On the other hand, doping can often change the particle morphology dramatically[5] and create mid-gap states essential for visible light activity of some wide-band-gap oxides.[21] In fact, the high activity of $NaTaO_3$ and the visible light activity of $SrTiO_3$ photocatalysts rely on such doping effects. Recently, much effort has been made to understand the effect of doping in terms of carrier dynamics.[22–24] From the material synthesis standpoint, the challenges in the activation of photocatalysts lie in how to lower defect densities, reduce particle sizes, and incorporate dopants effectively. The flux treatment of photocatalytic materials may offer a solution to such challenges.

$SrTiO_3$ is a classic photocatalyst that has been reported to be active in overall water splitting under UV light since 1980 (ref. 25 and 26) and is still widely investigated in fundamental studies on the effects of doping,[21,23,27,28] particle morphology,[29] and cocatalysts.[30] In a recent study, we found that doping of lower-valence cations in $SrTiO_3$, such as Na^+ into Sr^{2+} and Ga^{3+} into Ti^{4+}, dramatically enhanced the photocatalytic activity during the overall water splitting reaction.[27] We attributed the positive effect of doping to the lower density of trivalent Ti states. Thus, the effects of the incorporation of even a small amount of impurity into $SrTiO_3$ during the flux treatment should be carefully investigated.

In this paper, we studied the effects of $SrCl_2$ flux treatment and doping on the physical properties and photocatalytic activity of $SrTiO_3$. The crystallinity and water splitting activity of $SrTiO_3$ were dramatically improved by the flux treatment in alumina crucibles. A small amount of Al doped into $SrTiO_3$ from an alumina crucible was found to be responsible for the enhancement in photocatalytic activity. It was found that the external doping of Al in the presence of flux was the most effective for controlled Al doping and produced an apparent quantum efficiency exceeding 30% at 360 nm, the highest value reported so far in this wavelength region and on $SrTiO_3$ powder.

2 Experimental

Sample preparation

As-purchased $SrTiO_3$. $SrTiO_3$ (Wako Pure Chemicals Industries, Ltd, 99.9%) was employed as a raw material without any post-treatment (hereafter STO(pristine)).

Flux-treated $SrTiO_3$. $SrTiO_3$ (Wako Pure Chemicals Industries, Ltd, 99.9%), Al_2O_3 (Sigma-Aldrich Co, LLC., nanopowder), and $SrCl_2$ (Kanto Chemicals Co., Inc., 98.0%, anhydrous) were used as raw materials. $SrTiO_3$ and $SrCl_2$ were thoroughly mixed in an agate mortar. The mixture was heated either in a yttria or an alumina crucible at 1100 °C for 10 h. After the mixture was cooled to room temperature, $SrTiO_3$ was separated from the solidified mass by repeated washing with deionized water until no white AgCl precipitate formed in rinse solutions upon adding $AgNO_3$. The $SrTiO_3$ samples treated in yttria and alumina crucibles will hereafter be referred to as STO(flux-Y) and STO-(flux-Al), respectively, where -Y and -Al are used to highlight the material of the crucible used for the flux treatment. For STO(flux-Al), the same procedure was followed, except that heating was performed at 900 and 1000 °C instead of 1100 °C. For the synthesis of STO(flux-Y) with Al dopant, Al_2O_3 was mixed together with $SrTiO_3$ and $SrCl_2$ and the same procedure was followed subsequently. The STO(flux-Y) samples with Al_2O_3 addition will hereafter be referred to as x%Al-STO(flux-Y), where x% represents the Al/Ti molar ratio in the starting mixture.

Al-doped $SrTiO_3$. $SrTiO_3$ (Wako Pure Chemicals Industries, Ltd, 99.9%) and Al_2O_3 (Sigma-Aldrich Co, LLC., nanopowder) were thoroughly mixed in an agate mortar. The mixture was heated in an alumina crucible at 1100 °C for 10 h. These samples will hereafter be referred to as Al-STO(ssr-Y).

Deposition of cocatalyst. A mixed oxide of rhodium and chromium, $Rh_{2-y}Cr_yO_3$, was loaded as a cocatalyst by the impregnation method. The details of the method used have been described elsewhere.[31] The samples were loaded with $Na_3RhCl_6 \cdot nH_2O$ (Mitsuwa Chemistry Co., Ltd, Rh 17.8 wt%) and $Cr(NO_3)_3 \cdot 9H_2O$ (Kanto Chemicals Co., Inc., 98.0–103.0%) as Rh and Cr sources, respectively, and calcined in air at 350 °C for 1 h.

Measurement of photocatalytic activity

The activities of the photocatalyst samples were tested in a closed gas circulation system with a top-irradiation-type reactor. The deionized water (100 mL) was evacuated to remove air completely. The reactor was irradiated using a 300 W xenon lamp ($\lambda > 300$ nm) through a quartz window or using a 450 W high-pressure mercury lamp through a quartz cooling jacket and, when necessary, a 2 cm-diameter slit, a band pass filter ($\lambda = 360$ nm, FWHM = 10 nm), and a series of neutral density filters (OD = 0.3, 0.5, 1.0, and 2.0) to irradiate the sample with monochromatic light with controlled intensity. The evolved gases were analyzed by a gas chromatograph (Shimadzu, GC-8A) equipped with a thermal conductivity detector, using Ar as a carrier gas.

Sample characterization

The crystal structures of the products were characterized by X-ray diffractometry (XRD; RINT Ultima III, Rigaku Co.) using Cu K_α radiation at 40 kV and 40 mA. XRD peaks due to Cu $K_{\alpha1}$ and $K_{\alpha2}$ radiation were deconvoluted and the full width at half maximum (FWHM) of the (110) peak due to the Cu $K_{\alpha1}$ radiation was estimated. Specific surface areas were measured with a Belsorp-miniII (BEL Japan Inc.). The morphology of the powder was observed by scanning electron microscopy (SEM; S-4700, Hitachi High-Technologies Co.). Ultraviolet-visible diffuse reflectance spectrometry (DRS; V-670, Jasco Co.) was performed using spectralon (Jasco Co.) as a reference material. Inductively coupled plasma optical emission spectroscopy (ICP-OES; Shimadzu Co., ICPS-8100) was used for elemental analysis. $SrTiO_3$ powder (0.01 g) was melted with 1.0 g of a 3 : 1 mixture of Na_2CO_3 and $B(OH)_3$ by heating. An aqueous solution of tartaric acid (5%, 10 mL), HCl (1 + 1, 4 mL), and H_2O_2 (30 wt%, 1 mL) were added to dissolve the melt, and diluted with distilled water to make the total volume 100 mL. The resulting solution was used to measure Al and Y. The solution was further diluted tenfold to measure Sr and Ti.

3 Results and discussion

Commercially available $SrTiO_3$ (hereafter STO(pristine)) was mixed with $SrCl_2$ at a molar ratio of $SrCl_2/SrTiO_3 = 10$ and heated at 1100 °C for 10 h in yttria crucibles (hereafter STO(flux-Y)) and alumina crucibles (hereafter STO(flux-Al)) to obtain flux-treated $SrTiO_3$. X-ray diffraction (XRD) patterns are presented in Fig. 1. The XRD patterns for STO(flux-Y) and STO(flux-Al) showed only peaks attributable to the $SrTiO_3$ phase and exhibited sharper XRD peaks than STO(pristine), as reported in the literature.[24,29] The FWHM of the (110) XRD peak was 0.103 for STO(pristine) and it was reduced to 0.071 for STO(flux-Y) (Table 1). Under the same measurement conditions, the difference in the FWHM of XRD peaks reflects the difference in size and strain of crystallites. The reduction of the FWHM after the flux treatment should reflect the growth of crystallites with weaker strain, which is indicative of higher crystallinity.

The SEM images of the samples in Fig. 2 show that STO(pristine) consisted of particles with irregular shapes, a few hundred nanometers in size. The flux treatment changed the particle morphology dramatically. The STO(flux-Y) and STO(flux-Al) samples consisted of truncated cubic particles that exhibited a perovskite-type structure. The particles were 0.2–2 μm and 0.2–3 μm in size, respectively. The equilibrium crystal shape of $SrTiO_3$ was reported to be truncated cubic.[32] Since the flux treated STO crystals also consisted of truncated cubes, it is considered that these crystals exposed the surfaces with the lowest formation energy. The morphological change agreed well with the change in specific surface area of the samples. The BET surface area decreased upon flux treatment (Table 1). The BET surface area for STO(flux-Al) was slightly smaller than that for STO(flux-Y), agreeing well with the difference in their particle sizes.

Diffuse reflectance spectra (DRS) of the $SrTiO_3$ samples showed that their band gap was not changed by the flux treatments (Fig. S1 in the ESI†). The absorption edge was located at approximately 390 nm. Their indirect band gaps,[33,34] as estimated from the Tauc plots, were 3.2 eV, which well agreed with the reported values.[35]

Fig. 3 shows the water splitting activities of STO(pristine), STO(flux-Y) and STO(flux-Al). The water splitting activity of STO(pristine) roughly tripled upon $SrCl_2$ flux treatment in an yttria crucible (STO(flux-Y)). This is presumably due to the improvement in crystallinity. When the same $SrCl_2$ flux treatment was carried out on $SrTiO_3$ in an alumina crucible (STO(flux-Al)), the water splitting activity was enhanced much more significantly, reaching 550 H_2 μmol h^{-1} and 280 O_2 μmol h^{-1}. Our recent study on carrier dynamics in these $SrTiO_3$ powders conducted by time-resolved absorption (TA) spectroscopy revealed that most photoexcited electrons in STO(pristine) were deeply trapped, while those in STO(flux-Al) were in the conduction band or shallowly trapped.[24] This result well explains the enhanced water splitting activity of STO(flux-Al), because deeply trapped electrons would not be readily used for the hydrogen evolution reaction. STO(flux-Al) split water steadily for at least several hours, as shown in Fig. 4. The apparent quantum efficiency of STO(flux-Al) was measured to be 30% at 360 nm. This is much higher than the 4.3% reported for KCl-treated $SrTiO_3$, although the difference in reaction

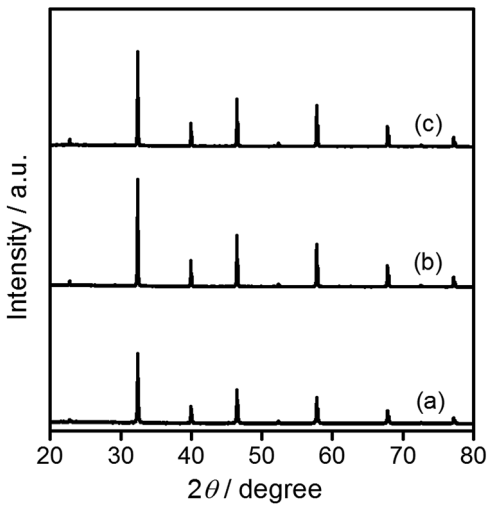

Fig. 1 XRD patterns for $SrTiO_3$ particles. (a) STO(pristine), (b) STO(flux-Y), and (c) STO(flux-Al).

Table 1 FWHM of the (110) diffraction peak, BET surface areas, and molar ratios, determined by ICP-OES of the $SrTiO_3$ photocatalysts

Sample	FWHM of (110) peak/°	BET surface area/m^2 g^{-1}	Molar ratio 2[Al]/([Sr] + [Ti])	Molar ratio 2[Y]/([Sr] + [Ti])
STO(pristine)	0.103	3.6	0.04%	0.00%
STO(flux-Y)	0.071	1.5	0.02%	0.48%
STO(flux-Al), 1100 °C	0.067	0.9	0.31%	0.00%
STO(flux-Al), 1000 °C	0.074	1.3	0.11%	0.01%
STO(flux-Al), 900 °C	0.084	1.9	0.12%	0.00%

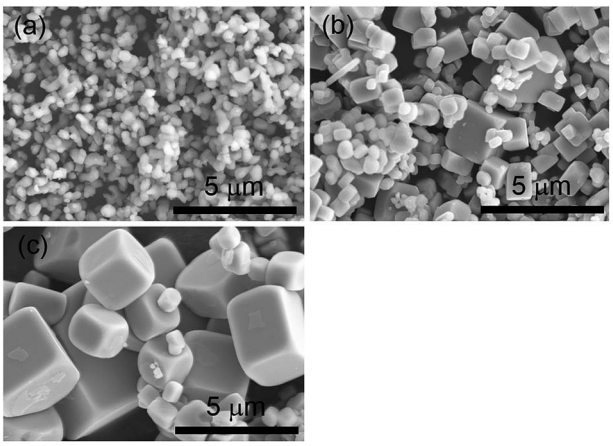

Fig. 2 SEM images of $SrTiO_3$ particles. (a) STO(pristine), (b) STO(flux-Y), and (c) STO(flux-Al).

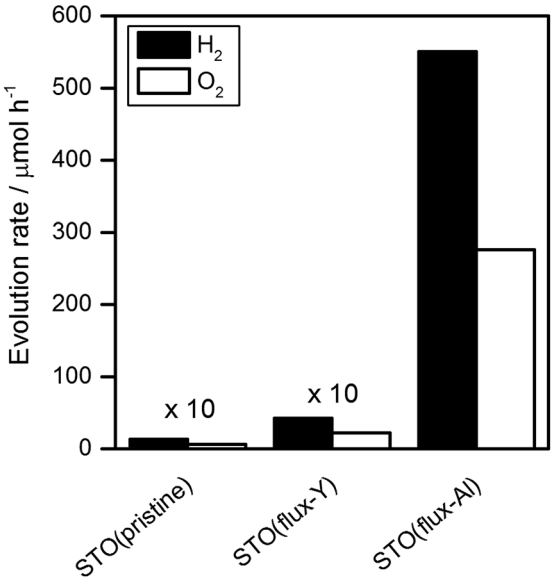

Fig. 3 Water splitting activity of $SrTiO_3$ photocatalysts. Reaction conditions: catalyst, 0.1 g; cocatalyst, $Rh_{2-y}Cr_yO_3$ (Rh 0.1 wt%, Cr 0.1 wt%); reaction solution, 100 mL H_2O; light source, 300 W Xe lamp ($\lambda > 300$ nm).

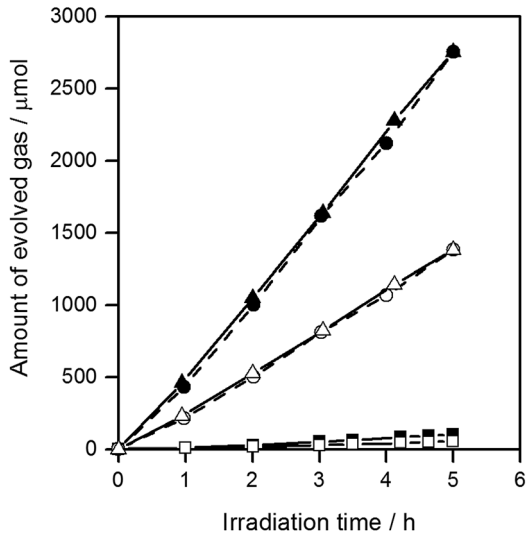

Fig. 4 Gas evolution during the water splitting reaction on STO(flux-Al). H_2 (■) and O_2 (□) on STO(flux-Al) treated at 900 °C, H_2 (●) and O_2 (○) on STO(flux-Al) treated at 1000 °C, and H_2 (▲) and O_2 (△) on STO(flux-Al) treated at 1100 °C. Reaction conditions: catalyst, 0.1 g; cocatalyst, $Rh_{2-y}Cr_yO_3$ (Rh 0.1 wt%, Cr 0.1 wt%); reaction solution, 100 mL H_2O; light source, 300 W Xe lamp ($\lambda > 300$ nm).

conditions should be taken into account.[29] We note that the apparent quantum efficiency was in fact dependent on the intensity of the incident light. As shown in Fig. S2 in the ESI,† the apparent quantum efficiency increased with light intensity under the experimental conditions examined. This result is not consistent with reaction orders to light intensity commonly observed in photocatalytic reactions, which is a first order.[36] We suspect that a certain kind of trap state with a limited density may have to be filled with photoexcited carriers to attain sufficient photoconductivity for charge separation. The kinetic interpretation of the light intensity dependence of the photocatalytic water splitting rate will be reported in follow-up studies.

The FWHM of the (110) XRD peak for STO(flux-Al) treated at 1100 °C and STO(flux-Y) were 0.067 and 0.071, respectively (Table 1). Therefore, the crystallinity of STO(flux-Al) treated at 1100 °C was higher than that of STO(flux-Y). This might explain the large difference in the enhancement of photocatalytic activity by $SrCl_2$ flux treatment in alumina and yttria crucibles. To determine the influence of crystallinity on the photocatalytic activity of flux-treated $SrTiO_3$, the crystallinity of STO(flux-Al) was controlled by increasing the treatment temperature above the melting point of $SrCl_2$ (874 °C). For treatment temperatures of 900–1100 °C, the XRD patterns for all samples were attributed to single-phase $SrTiO_3$, regardless of the treatment temperature (Fig. S3 in the ESI†). However, the FWHM of the (110) XRD peaks of STO(flux-Al) increased upon lowering the flux treatment temperature and became comparable to that of STO(flux-Y) (Table 1). The water splitting activity of STO(flux-Al) became markedly higher when the treatment temperature increased from 900 to 1000 °C (Fig. 4). This suggested that the improvement in water splitting activity of flux-treated $SrTiO_3$ was associated with improved crystallinity. However, STO(flux-Al) treated at 900 and 1000 °C exhibited a significantly higher water splitting rate than STO(flux-Y), although the crystallinity of the former was inferior. This points to a different, more predominant factor governing the water splitting activity of $SrTiO_3$.

We speculated that Al impurity, derived from the alumina crucibles, became incorporated into $SrTiO_3$ during flux treatment. Indeed, it has been reported that doping $SrTiO_3$ with lower-valence cations can boost its photocatalytic activity.[27] Therefore, an elemental analysis of the samples was carried out by inductively coupled plasma optical emission spectroscopy (ICP-OES). Table 1 tabulates the compositions of flux-treated $SrTiO_3$. Al ions, derived from the alumina crucibles, were indeed detected in the STO(flux-Al) samples, where they would replace the Ti^{4+} sites of $SrTiO_3$. As expected, STO(flux-Y) was free of Al, but instead, it was doped with Y from the yttria crucibles. The higher water splitting activity of STO(flux-Al) compared to STO(flux-Y) is thus most likely attributable to the effect of Al doping. The enhancement of the water splitting activity by doping lower valence cations is consistent with the recent studies[6,27,37] but contradictory to an earlier work on platinized doped TiO_2 systems.[38] The difference probably resulted from the cocatalysts used. The $Rh_{2-y}Cr_yO_3$ cocatalyst is known to block the reverse reaction, *i.e.*, formation of water from hydrogen and oxygen molecules, unlike noble metals which readily catalyze the reverse reaction.[31,39] Therefore, in this work, the water splitting activity is not obscured by the reverse reactions and closely reflects the change in the behavior of photoexcited charge carriers. Y doping did not have a significant positive effect on the photocatalytic activity. Unlike Al, Y presumably did not substitute well at the Ti sites because of the larger mismatch in ionic radius.

In an attempt to control Al doping in the presence of the $SrCl_2$ flux, $SrTiO_3$ and Al_2O_3 were mixed at molar ratios of

Al/Ti = 0.1%, 1%, and 10%, and heated together with the $SrCl_2$ flux in yttria crucibles. The resulting samples are referred to as *x*%Al-STO(flux-Y). The amount of Al doping was not directly proportional to the amount of Al_2O_3 added, but did increase with it (Table 2). In addition, certain amounts of Y were introduced from the yttria crucibles, similar to the case for the STO(flux-Y) sample. However, it is unlikely that Y doping at this level overwhelms the enhancement of photocatalytic activity by Al doping, considering the results for STO(flux-Y) (Fig. 3). The XRD patterns, SEM images, and BET surface areas for the samples and their water splitting activities are presented in Fig. S4 and S5 in the ESI,† Table 2, and Fig. 5, respectively. The 0.1%Al-STO(flux-Y) sample exhibited XRD patterns similar to those for STO(flux-Al). Single-phase $SrTiO_3$ was observed, and the FWHM of the (110) diffraction peak was 0.067. The morphology and BET surface area for 0.1%Al-STO(flux-Y) were also comparable to those for STO(flux-Al). However, the water splitting activity of 0.1%Al-STO(flux-Y) was much lower than that of STO(flux-Al) due to the lower Al content in 0.1%Al-STO(flux-Y) compared to STO(flux-Al). The particle size of 1%Al-STO(flux-Y) and 10%Al-STO(flux-Y) decreased upon Al addition and most of the particles lost their crystal facets, which were distinctive for STO(flux-Al) and STO(flux-Y). This change in morphology is presumably due to suppression of the crystal growth of $SrTiO_3$ by the excess Al_2O_3, similar to the case for $NaTaO_3$ doped with La.[5] A high activity for the overall water splitting reaction, comparable to that for STO(flux-Al), was obtained using yttria crucible when more than 1% of Al was added. This result supports our speculation that Al doping is the controlling factor for the enhancement of photocatalytic activity of $SrTiO_3$. On the other hand, the high activity of 10%Al-STO(flux-Y) despite its comparatively lower crystallinity may have resulted from the small particle sizes, which shorten the time needed for the migration of photoexcited carriers from the interior to the surface of photocatalyst particles.

Table 2 FWHM of the (110) diffraction peak, BET surface areas, and molar ratios, determined by ICP-OES of the $SrTiO_3$ photocatalysts

			Molar ratio	
Sample	FWHM of (110) peak/°	BET surface area/m^2 g^{-1}	2[Al]/([Sr] + [Ti])	2[Y]/([Sr] + [Ti])
0.1%Al-STO(flux-Y)	0.067	0.9	0.12%	0.16%
1%Al-STO(flux-Y)	0.096	2.7	1.01%	0.70%
10%Al-STO(flux-Y)	0.091	2.4	1.36%	0.57%
0.1%Al-STO(ssr-Y)	0.077	1.7	0.10%	0.00%
1%Al-STO(ssr-Y)	0.094	3.0	1.07%	0.00%
5%Al-STO(ssr-Y)	0.095	3.7	4.24%	0.01%
10%Al-STO(ssr-Y)	0.096	3.9	8.25%	0.01%

To examine the effect of aluminum doping separately, Al_2O_3 was added as a dopant to $SrTiO_3$ at Al/Ti molar ratios ranging from 0.1% to 10%, and the mixtures were calcined in the absence of the $SrCl_2$ flux for a solid state reaction. The resulting products are referred to as *x*%Al-STO(ssr-Y), where *x*% represents the Al/Ti molar ratio in the starting mixture. As tabulated in Table 2, the Al content increased monotonically with increasing amount of Al_2O_3 addition, although the amounts detected were somehow lower than the amounts added to the starting material for high Al_2O_3 contents (Al >5%). The amount of Al incorporated into $SrTiO_3$ had a significant influence on the water splitting activity of the resulting samples. The water splitting activity peaked for 0.1%Al-STO(ssr-Y), as shown in Fig. 6. The activity of 0.1%Al-STO(ssr-Y) was two orders of magnitude higher than that of STO(pristine), but lower than that of STO(flux-Al) (Fig. 3). At this doping amount, no impurity

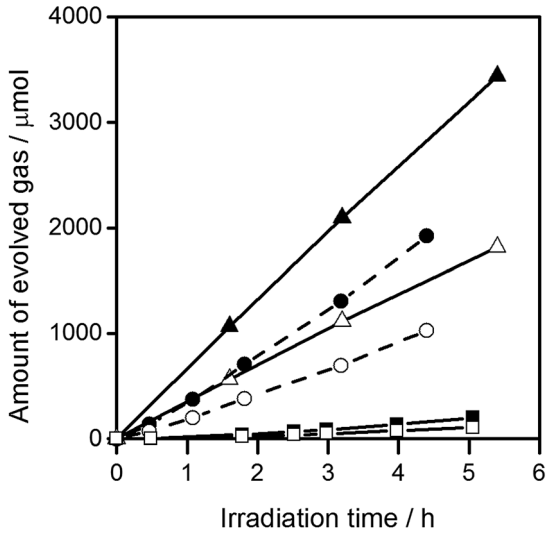

Fig. 5 Gas evolution during the water splitting reaction on Al-STO(-flux-Y). H_2 (■) and O_2 (□) on 0.1%Al-STO(flux-Y), H_2 (●) and O_2 (○) on 1%Al-STO(flux-Y), and H_2 (▲) and O_2 (△) on 10%Al-STO(flux-Y). Reaction conditions: catalyst, 0.1 g; cocatalyst, $Rh_{2-y}Cr_yO_3$ (Rh 0.1 wt%, Cr 0.1 wt%); reaction solution, 100 mL H_2O; light source, 300 W Xe lamp (λ > 300 nm).

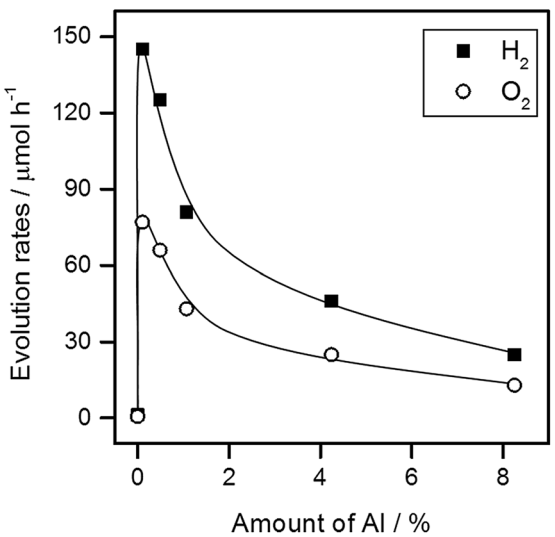

Fig. 6 Dependence of the water splitting activity of STO(ssr-Y) on the amount of Al doping. Reaction conditions: catalyst, 0.1 g; cocatalyst, $Rh_{2-y}Cr_yO_3$ (Rh 0.1 wt%, Cr 0.1 wt%); reaction solution, 100 mL H_2O; light source, 300 W Xe lamp (λ > 300 nm).

phase was detected in the XRD patterns of the sample (Fig. S6†). The BET surface area for 0.1%Al-STO(ssr-Y) decreased to 1.7 $m^2\ g^{-1}$ owing to the sintering process. However, it should be noted that no significant difference in morphology was observed between STO(pristine) and *x*%Al-STO(ssr-Y) (Fig. S7†). These results corroborate the necessity of the $SrCl_2$ flux for morphological change. It is worth mentioning that the impurity concentration that can dramatically improve the water splitting activity of $SrTiO_3$ (~0.1 mol%) is close to the detection limits of commonly employed methods for elemental analysis, such as energy-dispersive X-ray emission spectroscopy (EDS) and X-ray photoelectron spectroscopy (XPS). Therefore, extra care needs to be taken when the effects of flux treatment on photocatalytic properties are discussed.

It should be noted that Al doping of $SrTiO_3$ was more effective when $SrCl_2$ was present during the heating. The doping amount of Al in the STO(flux-Al) sample from an alumina crucible may vary depending on the treatment conditions. Nevertheless, this sample showed a higher photocatalytic activity than the Al-STO(ssr-Y) samples containing various and controlled amounts of Al. It is thought that Al was not effectively doped into $SrTiO_3$ during the solid state reaction because Al had to diffuse from the outer surface of the particles. In contrast, a significant portion of the $SrTiO_3$ particles was once dissolved and recrystallized in the presence of $SrCl_2$ flux, together with alumina derived from the crucibles. During this process, some of the Al ions may be doped into the middle part of the $SrTiO_3$ particles and occupy the most stable state thermodynamically. As a result, Al doping can show stronger enhancement of photocatalytic activity when the $SrCl_2$ flux is used. Thus, it is concluded that the dramatic improvement in the photocatalytic activity of STO(flux-Al) was due to Al doping and the enhancement of crystallinity observed upon flux treatment.

4 Conclusions

The photocatalytic activity of $SrTiO_3$ in the overall water splitting reaction was dramatically improved by $SrCl_2$ flux treatment at 1100 °C in an alumina crucible. The improvement in activity was attributed mainly to the doping of Al derived from the crucibles. The morphological change and the enhanced crystallinity also improved the photocatalytic activity, although these factors were found to be less significant than the effect of Al doping on the basis of the results of flux treatment in Al-free conditions. It was confirmed that $SrTiO_3$ doped with Al under a $SrCl_2$ flux showed even higher water splitting activity than $SrTiO_3$ doped with Al by a solid state reaction. It is believed that the flux worked as a medium to dissolve the Al_2O_3 dopant and the host $SrTiO_3$ particles, facilitating the Al doping of $SrTiO_3$. As a consequence, the apparent quantum efficiency in overall water splitting was increased to 30% at 360 nm. Flux-mediated doping is expected to greatly broaden the possibilities of photocatalytic materials by activating them under visible light irradiation. In addition, the incorporation of impurities into the samples during flux treatment was a common occurrence and could have strong impact on the photocatalytic activity. Therefore, particular attention should be paid to flux treatment of photocatalysts.

5 Acknowledgements

This work was financially supported by Grants-in-Aid for Specially Promoted Research (No. 23000009) and for Young Scientists (A) (No. 15H05494), and the A3 Foresight Program of Japan Society for the Promotion of Science (JSPS). The authors thank Dr Taro Yamada in The University of Tokyo for his kind cooperation with ICP-OES.

References

1 A. Kudo and Y. Miseki, *Chem. Soc. Rev.*, 2009, **38**, 253–278.
2 X. Chen, S. Shen, L. Guo and S. S. Mao, *Chem. Rev.*, 2010, **110**, 6503–6570.
3 K. Maeda and K. Domen, *J. Phys. Chem. Lett.*, 2010, **1**, 2655–2661.
4 T. Hisatomi, K. Takanabe and K. Domen, *Catal. Lett.*, 2015, **145**, 95–108.
5 H. Kato, K. Asakura and A. Kudo, *J. Am. Chem. Soc.*, 2003, **125**, 3082–3089.
6 Y. Sakata, Y. Matsuda, T. Nakagawa, R. Yasunaga, H. Imamura and K. Teramura, *ChemSusChem*, 2011, **4**, 181–184.
7 K. Sayama, A. Tanaka, K. Domen, K. Maruya and T. Onishi, *Catal. Lett.*, 1990, **4**, 217–222.
8 K. Sayama, A. Tanaka, K. Domen, K. Maruya and T. Onishi, *J. Catal.*, 1990, **124**, 541–547.
9 T. Takata, Y. Furumi, K. Shinohara, A. Tanaka, M. Hara, J. N. Kondo and K. Domen, *Chem. Mater.*, 1997, **9**, 1063–1064.
10 B. A. Pinaud, J. D. Benck, L. C. Seitz, A. J. Forman, Z. Chen, T. G. Deutsch, B. D. James, K. N. Baum, G. N. Baum, S. Ardo, H. Wang, E. Miller and F. Jaramillo Thomas, *Energy Environ. Sci.*, 2013, **6**, 1983–2002.
11 M. Schieber, *J. Am. Ceram. Soc.*, 1964, **47**, 537–538.
12 K. Teshima, K. Horita, T. Suzuki, N. Ishizawa and S. Oishi, *Chem. Mater.*, 2006, **18**, 3693–3697.
13 S. Suzuki, K. Teshima, A. Yamaguchi, K. Yubuta, T. Shishido and S. Oishi, *CrystEngComm*, 2012, **14**, 987–992.
14 K. Teshima, K. Yubuta, T. Shimodaira, T. Suzuki, M. Endo, T. Shishido and S. Oishi, *Cryst. Growth Des.*, 2008, **8**, 465–469.
15 H. Yoshida, M. Takeuchi, M. Sato, L. Zhang, T. Teshima and M. G. Chaskar, *Catal. Today*, 2014, **232**, 158–164.
16 D. Noureldine, D. H. Anjum and K. Takanabe, *Phys. Chem. Chem. Phys.*, 2014, **16**, 10762–10769.
17 F. Zhang, A. Yamakata, K. Maeda, Y. Moriya, T. Takata, J. Kubota, K. Teshima, S. Oishi and K. Domen, *J. Am. Chem. Soc.*, 2012, **134**, 8348–8351.
18 M. J. Bojdys, J.-O. Müller, M. Antonietti and A. Thomas, *Chem.–Eur. J.*, 2008, **14**, 8177–8182.
19 T. Takata, D. Lu and K. Domen, *Cryst. Growth Des.*, 2010, **11**, 33–38.
20 G. Muller, A. Ostrogorsky and D. Hurle, *Basic Techniques*, 1994, vol. 2, pp. 573–574.

21 R. Asai, H. Nemoto, Q. Jia, K. Saito, A. Iwase and A. Kudo, *Chem.Commun.*, 2014, **50**, 2543–2546.
22 M. Maruyama, A. Iwase, H. Kato, A. Kudo and H. Onishi, *J. Phys. Chem. C*, 2009, **113**, 13918–13923.
23 K. Furuhashi, Q. Jia, A. Kudo and H. Onishi, *J. Phys. Chem. C*, 2013, **117**, 19101–19106.
24 A. Yamakata, H. Yeilin, M. Kawaguchi, T. Hisatomi, J. Kubota, Y. Sakata and K. Domen, *J. Photochem. Photobiol., A*, 2015, DOI: 10.1016/j.jphotochem.2015.05.016.
25 K. Domen, S. Naito, M. Soma, T. Onishi and K. Tamaru, *J. Chem. Soc., Chem. Commun.*, 1980, 543–544.
26 K. Domen, A. Kudo, T. Onishi, N. Kosugi and H. Kuroda, *J. Phys. Chem.*, 1986, **90**, 292–295.
27 T. Takata and K. Domen, *J. Phys. Chem. C*, 2009, **113**, 19386–19388.
28 Q. Wang, T. Hisatomi, S. S. K. Ma, Y. Li and K. Domen, *Chem. Mater.*, 2014, **26**, 4144–4150.
29 H. Kato, M. Kobayashi, M. Hara and M. Kakihana, *Catal. Sci. Technol.*, 2013, **3**, 1733–1738.
30 T. K. Townsend, N. D. Browning and F. E. Osterloh, *Energy Environ. Sci.*, 2012, **5**, 9543–9550.
31 K. Maeda, K. Teramura, H. Masuda, T. Takata, N. Saito, Y. Inoue and K. Domen, *J. Phys. Chem. B*, 2006, **110**, 13107–13112.
32 T. Sano, D. M. Saylor and G. S. Rohrer, *J. Am. Ceram. Soc.*, 2003, **86**, 1933–1939.
33 A. Kahn and A. Leyendecker, *Phys. Rev.*, 1964, **135**, A1321.
34 M. Capizzi and A. Frova, *Phys. Rev. Lett.*, 1970, **25**, 1298.
35 K. van Benthem, C. Elsässer and R. French, *J. Appl. Phys.*, 2001, **90**, 6156–6164.
36 T. Hisatomi, K. Maeda, K. Takanabe, J. Kubota and K. Domen, *J. Phys. Chem. C*, 2009, **113**, 21458–21466.
37 K. Maeda, D. Lu and K. Domen, *Chem.–Eur. J.*, 2013, **19**, 4986–4991.
38 K. E. Karakitsou and X. E. Verykios, *J. Phys. Chem.*, 1993, **97**, 1184–1189.
39 K. Maeda, K. Teramura, D. Lu, N. Saito, Y. Inoue and K. Domen, *Angew. Chem.*, 2006, **118**, 7970–7973.